



Active Power Control for Wind Farms Using Distributed Model Predictive Control and Nearest Neighbor Communication

Preprint

Christopher Bay and Timothy Taylor
Colorado School of Mines

Jennifer Annoni and Kathryn Johnson
National Renewable Energy Laboratory

Lucy Pao
University of Colorado, Boulder

*Presented at the American Control Conference
Milwaukee, Wisconsin
June 27–29, 2018*

Suggested Citation

Bay, Christopher, Jennifer Annoni, Kathryn Johnson, and Lucy Pao. 2018. "Active Power Control for Wind Farms Using Distributed Model Predictive Control and Nearest Neighbor Communication: Preprint." Golden, CO: National Renewable Energy Laboratory. NREL/CP-5000-70936. <https://www.nrel.gov/docs/fy18osti/70936>.

**NREL is a national laboratory of the U.S. Department of Energy
Office of Energy Efficiency & Renewable Energy
Operated by the Alliance for Sustainable Energy, LLC**

This report is available at no cost from the National Renewable Energy Laboratory (NREL) at www.nrel.gov/publications.

Conference Paper
NREL/CP-5000-70936
August 2018

Contract No. DE-AC36-08GO28308

NOTICE

This work was authored in part by the National Renewable Energy Laboratory, operated by Alliance for Sustainable Energy, LLC, for the U.S. Department of Energy (DOE) under Contract No. DE-AC36-08GO28308. Funding provided by the U.S. Department of Energy Office of Energy Efficiency and Renewable Energy Wind Energy Technologies Office. The views expressed in the article do not necessarily represent the views of the DOE or the U.S. Government. The U.S. Government retains and the publisher, by accepting the article for publication, acknowledges that the U.S. Government retains a nonexclusive, paid-up, irrevocable, worldwide license to publish or reproduce the published form of this work, or allow others to do so, for U.S. Government purposes.

This report is available at no cost from the National Renewable Energy Laboratory (NREL) at www.nrel.gov/publications.

U.S. Department of Energy (DOE) reports produced after 1991 and a growing number of pre-1991 documents are available free via www.OSTI.gov.

Cover Photos by Dennis Schroeder: (left to right) NREL 26173, NREL 18302, NREL 19758, NREL 29642, NREL 19795.

NREL prints on paper that contains recycled content.

Active Power Control for Wind Farms Using Distributed Model Predictive Control and Nearest Neighbor Communication

Christopher J. Bay,^{1,3} Jennifer Annoni,² Timothy Taylor,¹ Lucy Pao,³ and Kathryn Johnson^{1,2}

Abstract—Wind plant control strategies, including axial induction and wake steering control, aim to improve the performance of wind farms, including increasing energy production and decreasing turbine loads. This paper presents a linear model of wake characteristics for use with a distributed model predictive control method for the purpose of optimizing axial induction and yaw misalignment setpoints. In particular, we use an iterative, distributed control method with nearest neighbor communication to coordinate turbine control actions that account for wake interactions between turbines. Simulations of the model and controller are performed on a 2×3 array of turbines using a modified version of the FLOW Redirection and Induction in Steady-state (FLORIS) model to dynamically track the relevant wake parameters. Preliminary results show the controller’s ability to follow an arbitrary wind farm power reference signal for the purpose of providing active power control (APC) ancillary services for power grid stability. This efficient distributed control strategy can enable real-time wind farm optimization and control, even for very large scale farms.

I. INTRODUCTION

Wind energy has remained a consistent focus of renewable energy development with installed global capacity increasing by five-fold over the last decade [1]. As wind provides more and more of the energy the world consumes, opportunities remain to further decrease the levelized cost of wind energy, increasing its competitiveness with traditional sources. This has led to significant research into effective wind turbine operation and control with a recent focus into control at the wind farm level. The goals of these efforts have included structural load reductions to increase equipment life, maximization of power production, and more robust integration of wind into the energy grid [2], [3].

*This work has been partially supported by ARPA-E under award number DE-AR0000667, the German Academic Exchange Service (DAAD) with funds from the Federal Ministry of Education and Research (BMBF), Envision Energy, and the National Science Foundation under Grant No. NSF-CMMI-1234980. In addition, this work was supported by the U.S. Department of Energy under Contract No. DE-AC36-08GO28308 with the National Renewable Energy Laboratory. Funding for the work was provided by the DOE Office of Energy Efficiency and Renewable Energy, Wind Energy Technologies Office. The U.S. Government retains and the publisher, by accepting the article for publication, acknowledges that the U.S. Government retains a nonexclusive, paid-up, irrevocable, worldwide license to publish or reproduce the published form of this work, or allow others to do so, for U.S. Government purposes. The authors are solely responsible for any omission or errors contained herein. Any opinions, findings, and conclusions or recommendations expressed in this material are those of the author(s) and do not necessarily reflect the views of the funding agencies.

C. J. Bay is a post-doctoral researcher at the Colorado School of Mines and University of Colorado Boulder (e-mail: christopher.j.bay@gmail.com).¹Electrical Engineering Department, Colorado School of Mines, Golden, CO 80401 USA. ²National Renewable Energy Laboratory, Golden, CO 80401 USA. ³Electrical, Computer, & Energy Engineering, University of Colorado, Boulder, CO, 80309.

A recent area of interest has been turbine wake control. As wind turbines extract power, wind speeds are reduced and turbulence is increased within the wakes. The reduced speeds decrease the potential power that can be produced at the downstream turbines, resulting in suboptimal power production for the wind farm. One strategy to coordinate the wakes has been through axial induction control [4], [5]. Upstream turbines reduce their energy capture so that greater wind energy and less turbulence reach the downstream systems. Another strategy includes wake steering [6], [7]. Wake steering involves misaligning the rotor of the turbine with the incoming wind direction to deflect the wakes away from downstream turbines.

Additionally, there has been growing interest in active power control (APC), in which the wind farm manages its power output in accordance with requirements from the grid. There are many types of APC [8], but one example is automatic generation control (AGC). In AGC, a wind farm tracks a power reference signal typically given by a transmission system operator (TSO). This tracking can help balance the electrical grid or provide a power reserve allowing for quicker responses to changes in demand beyond traditional power generation equipment.

To accomplish these strategies, several control methods have been proposed. One study evaluated combinations of torque and pitch control, coupled with static optimal yaw setpoints, to track a power reference signal across the wind farm [9]. The authors concluded that a wake model is needed to predict the available power in the wind more effectively. The authors of [10] expand on the work of [9] and propose a gain-scheduled proportional-integral controller as a closed-loop supervisory solution to distribute the power reference among turbines. The authors showed improved tracking behavior for the total power output of the farm in highly waked cases.

Gionfra, et al. [11], examined the available power gain when using a wake model with model predictive control (MPC) to represent the interactions between turbines. Although this work includes a wake model in the central controller, it focuses on axial induction and ignores the effects of wake steering. Vali et al. [12] also used MPC with an adjoint-based approach, similar to [13], for computing the gradient of the system, where they sought to maximize power. Even though the authors use an efficient adjoint method, the authors keep measurements of the entire wind field that can become cumbersome as the size of wind farms grow. The authors also only consider axial induction control.

Another MPC approach aims to provide secondary fre-

quency regulation for the grid by optimizing thrust coefficients of individual turbines [14]. To enable real-time implementation, the method utilizes a time-varying one-dimensional wake model in which rows of turbines are considered to behave similarly. This assumption greatly speeds the computation but neglects differences in the incoming wind profiles. This assumption also requires turbines to be fully waked, which eliminates wake steering and is only valid for limited wind directions.

Nearly all of the aforementioned control solutions require a centralized controller, which can become infeasible as the size of a wind farm grows. One potential solution is to distribute the problem into smaller subsystems. Additionally, this eliminates single points of failure and increases modularity as turbines are maintained or repaired. However, there has been very little work completed in the area of distributed wind farm controls. The work by Spudić et al. [15] proposed using two distributed optimization methods to provide power reference tracking and structural load reduction. While the results are promising, the solution does not use a wake model and requires a global problem to be formulated. Also, [16] used a linearized flow field with an H_2 optimal distributed controller; however, the method is computationally complex and not suitable for large wind farms.

In this paper, a distributed model predictive control (DMPC) method, known as Limited-Communication DMPC (LC-DMPC) [17], is applied to the wind farm control problem. A linear model, including time-varying axial induction factors, yaw misalignments, and wake characteristics, is described and used by the LC-DMPC method to determine optimal axial induction and yaw control actions. A key contribution of this formulation is that it does not require a centralized model or problem formulation, as each subsystem solves its own local objective function. Each subsystem need only communicate with its nearest neighbor. Preliminary simulation results are presented showing the controller's ability to track an arbitrary power reference signal.

The main contributions of this paper are the development of a novel linear wind farm model that includes wake characteristics and the formulation of the wind farm control problem that optimizes axial induction and yaw misalignment in a dynamic, distributed fashion.

The rest of the paper is organized as follows. Section II presents the developed wake model for the control problem. The control structure is detailed in Section III. Simulation of the proposed method is performed on a 2×3 turbine grid and is described in Section IV. Preliminary results are presented in Section V. Lastly, conclusions and future work are discussed in Section VI.

II. WAKE MODEL

As mentioned in Section I, turbines can have significant impacts on each other through wake interactions. As an upwind turbine extracts power, the wind velocity that the downstream turbine sees is reduced and turbulent structures are introduced into the wake. To effectively control for these effects at the wind farm level, a suitable wake model

is needed. What follows is a derivation of a wake model to enable the use of the LC-DMPC algorithm as well as practical computational efficiency for implementation.

A. Wake Deflection

When a turbine is yawed away from the incoming wind direction, the rotor causes a deflection in the turbine's wake away from the downstream centerline behind the turbine. Jimenez, et al. [18] proposed an empirical correction for the wake deflection based on the yaw error, θ , and the thrust, C_T . First, the angle of wake deflection, α , is defined as:

$$\alpha = \frac{\cos^2(\theta_u) \sin(\theta_u) C_{T,u}}{2 \left(1 + k_d \left(\frac{x}{D}\right)\right)^2} \quad (1)$$

where k_d is the wake deflection coefficient, x is the distance downstream between the interacting turbines, and D is the rotor diameter assumed to be constant across the wind farm. The yaw misalignment and thrust coefficient from the upstream turbine are represented as θ_u and $C_{T,u}$, where u denotes values from the upwind turbine. From actuator disk theory, the thrust coefficient can be defined as a quadratic relationship dependent on axial induction factor a [19]:

$$C_{T,u} = 4a_u(1 - a_u) \quad (2)$$

Using the small angle approximation, the wake deflection can be approximated by $\delta = \alpha x$. Also, two approximations are made to further linearize the system:

$$\cos^2(\theta_u) \sin(\theta_u) \approx 0.125\theta_u \quad C_{T,u} \approx 3.0a_u \quad (3)$$

where the first approximation is valid up to 15° of yaw misalignment. Substituting (1) and (3) into $\delta = \alpha x$, the wake deflection is:

$$\delta = \frac{0.125\theta_u 3.0a_u}{2 \left(1 + k_e \left(\frac{x}{D}\right)\right)^2} x \quad (4)$$

Equation (4) can be represented as:

$$\delta = c_1 \theta_u c_2 a_u \quad (5)$$

where the constants c_1 and c_2 are defined as:

$$c_1 = 0.0125 \quad c_2 = \frac{3.0x}{2 \left(1 + k \left(\frac{x}{D}\right)\right)^2} \quad (6)$$

With $\delta(t)$, $\theta(t)$, and $a(t)$, Equation (5) can be written as:

$$\delta(t) = c_1 \theta_u(t - \tau) c_2 a_u(t - \tau) \quad (7)$$

where τ is the amount of time it takes for the effects of the control actions of the upstream turbine to reach the downstream turbine. Using Taylor's frozen turbulence hypothesis [20], it is assumed that τ is:

$$\tau = \frac{x}{U_\infty} \quad (8)$$

where U_∞ is the freestream velocity and it is assumed that the flow is advected at this speed. Lastly, after taking the derivative, linearizing about $\theta_u = 0$ and a nonzero axial induction factor \bar{a}_u , and discretizing, the equation for wake deflection becomes:

$$\delta^{k+1} = \delta^k + c_1 c_2 \bar{a}_u (\theta_u^k - \theta_u^{k-1}) \quad (9)$$

where the superscript k denotes the discrete timestep, the size of which is equal to τ . This value of τ is chosen to use the least amount of states as possible for this model. In future work, smaller timesteps will be considered.

B. Wake Width

As turbine wakes move downstream, the wake width expands. This is due to a rotation induced on the wake from the opposing force generated by the rotor blades on the air. Bastankhah and Porté-Agel [21] define the wake width as a linear expansion based on turbulence theory:

$$\sigma = k_y x + D \sqrt{\frac{1}{8}} \quad (10)$$

where k_y is the wake expansion coefficient, defined in terms of turbulence intensity, T_o , the upstream axial induction factor, a_u , and the downstream distance, x , between turbines:

$$k_y = 1.4T_o^{0.1} \left(\frac{x}{D}\right)^{-0.1} a_u + 0.004 \quad (11)$$

where 1.4, 0.1, and -0.1 are empirical constants tuned for this model. With (11), (10) becomes:

$$\sigma(t) = c_3 a_u (t - \tau) + c_4 \quad (12)$$

$$c_3 = 1.4T_o^{0.1} \left(\frac{x}{D}\right)^{-0.1} x \quad c_4 = 0.004x + D \sqrt{\frac{1}{8}} \quad (13)$$

Taking the derivative and discretizing provides:

$$\sigma^{k+1} = \sigma^k + c_3 (a_u^{k-N} - a_u^{k-N-1}) \quad (14)$$

C. Wake Centerline Velocity

The wake centerline velocity is defined using the Park/Jensen model [22]:

$$u = U_\infty \left(1 - 2a_u \left(\frac{D}{D + 2k_e x}\right)^2\right) \quad (15)$$

Equation 15 can be written as:

$$u(t) = c_5 + c_6 a_u (t - \tau) \quad (16)$$

$$c_5 = U_\infty \quad c_6 = -2U_\infty \left(\left(\frac{D}{D + 2k_e x}\right)^2\right) \quad (17)$$

where k_e is the wake expansion coefficient, different from k_y . Again, taking the derivative and discretizing gives a linear form of the equation suitable for the LC-DMPC control method:

$$u^{k+1} = u^k + c_6 (a_u^{k-N} - a_u^{k-N-1}) \quad (18)$$

D. Yaw and Thrust Control Models

To simulate the dynamics of the local yaw and thrust controllers, simple proportional controllers are used for each. The discrete time yaw and thrust controllers are given by:

$$\theta_S^{k+1} = \theta_S^k + K_\theta (\theta_S^k - \theta_{S,r}) \quad (19)$$

$$a_S^{k+1} = a_S^k + K_a (a_S^k - a_{S,r}) \quad (20)$$

where θ_r is the reference to the yaw controllers, a_r is the reference to the thrust controllers, and S is either u or d for upstream or downstream systems. Future work will include more sophisticated PID controllers for these local actions.

E. Power Output

The output of the model is the power produced by each turbine. Starting with the nonlinear computation of the effective velocity used in FLORIS [23], a simplification of the area overlap of a wake with the rotor disk can be made to calculate the effective velocity as:

$$U_d^k = \left(1 + \frac{\delta^k - Y}{\sigma^k}\right) u^k \quad (21)$$

where Y is the relative difference between the y locations of the upstream and downstream turbines. The linearization of (21) is valid up to 15° of yaw. With (21), a linearized power equation can be obtained. Turbine power is defined as:

$$P^k = \frac{1}{2} \rho A C_{P,d}^k \cos^2(\theta_d^k) (U_d^k)^3 \quad (22)$$

where ρ is the air density and A is the swept rotor area. The power coefficient can be defined as $C_P = 4\eta a(1-a)^2$, where $\eta = 0.8$ is a correction term defined by Gebraad [7].

Linearizing (22) about the operating point $\bar{\theta}_{u,d} = 0^\circ$ would result in the $\bar{\theta}_d$ term going to zero due to a $\sin(\theta)$, which is undesirable. As such, an approximation was made for the linearization term associated with $\bar{\theta}_d$ such that $\cos^2(\bar{\theta}_d) \approx (1 - 0.002\bar{\theta}_d)$. Under this assumption, the model is only valid for yaw control over $[0^\circ, 15^\circ]$. With the above approximation, the linearization of (22) gives:

$$\begin{aligned} P^k &= \frac{1}{2} \epsilon U_{eff}^3 + \frac{3}{2} \epsilon \zeta \frac{U_{eff}}{\bar{\sigma}} (\delta^k - \bar{\delta}) \\ &+ \frac{3}{2} \epsilon \zeta \left[\frac{U_{eff}(Y - \bar{\delta})}{\bar{\sigma}^2} \right] (\sigma^k - \bar{\sigma}) \\ &+ \frac{3}{2} \epsilon \zeta \left[1 + \frac{\bar{\delta} - Y}{\bar{\sigma}} \right] (u^k - U_{eff}) \\ &+ \frac{1}{2} \rho A \cos^2(\bar{\theta}_d) U_{eff}^3 [12\bar{a}_d^2 - 16\bar{a}_d + 4] (a_d^k - \bar{a}_d) \\ &- \frac{1}{10} \rho A [4\eta \bar{a}_d (1 - \bar{a}_d)^2] U_{eff}^3 (\theta_d^k - \bar{\theta}_d) \end{aligned} \quad (23)$$

where ϵ and ζ are defined as:

$$\epsilon = \rho A [4\eta \bar{a}_d (1 - \bar{a}_d)^2] \cos^2(\bar{\theta}_d) \quad (24)$$

$$\zeta = \left[\left(1 + \frac{\bar{\delta} - Y}{\bar{\sigma}}\right) U_{eff} \right]^2 \quad (25)$$

and U_{eff} is the effective rotor speed as calculated by FLORIS. In the next section, (9), (14), (18), (19), (20), and (23) will be composed into a linear state-space model.

III. DISTRIBUTED CONTROL STRUCTURE

As mentioned in Section I, a distributed model predictive controller is used to optimize the wind farm performance. The specific algorithm used is Limited-Communication DMPC (LC-DMPC), presented in [17]) is an iterative, cooperative algorithm for linear discrete time systems. Where it stands out is that for it to converge, only directly coupled subsystems need to share local information and adjust their

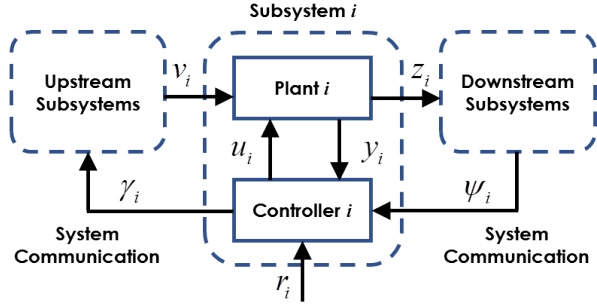


Fig. 1. Hierarchy for LC-DMPC algorithm [17].

actions accordingly without a solution of a centralized problem. A brief explanation of the algorithm will be included here and the reader is referred to [17] for more details.

Fig. 1 shows an overview of the LC-DMPC structure. The overall system is organized into subsystems that consist of plants, which in the case of wind farms are individual turbines and their local controllers. During an iteration, the local subsystem, i , shares its predicted effects, z_i , with its downstream neighbors and receives its upstream neighbors' effects as a disturbance vector, v_i . These effects are used to calculate sensitivities, γ_{i+1} , of the downstream system to the upstream system's actions, and these sensitivities are then passed to the upstream systems, as ψ_i , on the next iteration. The subsystem then solves the updated local optimization using the sensitivities and communicates its new effects to the downstream systems for the next iteration.

A. Linear State-Space Model

For the LC-DMPC algorithm, the system equations must be in a linear state-space representation of the form:

$$\begin{aligned} x_i^{k+1} &= A_i x_i^k + B_{u,i} u_i^k + B_{v,i} v_i^k \\ y_i^k &= C_{y,i} x_i^k \\ z_i^k &= C_{z,i} x_i^k + D_{z,i} u_i^k \end{aligned} \quad (26)$$

where x_i^k are the states, u_i^k are the control inputs, and v_i^k is the disturbance vector from upstream systems. The state equation is defined in (27). The output of the local plant y_i^k is power, given by (28). The vector containing disturbing effects for downstream systems is z_i^k given in (29).

Equations (9), (14), (19), and (20) were used to generate the state matrices A_i , $B_{u,i}$, and $B_{v,i}$ as shown in Equation (27), where K_θ and K_a are the proportional gains for the yaw and axial induction controllers, respectively. The constants $c_{1,i}$, $c_{2,i}$, $c_{3,i}$, and $c_{6,i}$ are derived from the linearized, discrete equations and are defined in (6), (13), and (17).

$$C_{y,i} = \left[\frac{3}{2} \epsilon_i \zeta_i \frac{U_{eff}}{\sigma_i} \quad \frac{3}{2} \epsilon_i \zeta_i \frac{(Y_i - \bar{\delta}_i) U_{eff}}{\sigma_i^2} \quad -\frac{3}{2} \epsilon_i \zeta_i \left[1 + \frac{\bar{\delta}_i - Y_i}{\sigma_i} \right] \quad -\frac{2}{5} \rho A \eta \bar{a}_d (1 - \bar{a}_d)^2 U_{eff}^3 \quad 0 \quad \frac{1}{2} \rho A \cos^2(\bar{\theta}_d) (12 \bar{a}_i^2 - 16 \bar{a}_i + 4) U_{eff}^3 \quad 0 \right] \quad (28)$$

$$\begin{aligned} \underbrace{\begin{bmatrix} \delta_i^{k+1} \\ \sigma_i^{k+1} \\ u_i^{k+1} \\ \theta_i^{k+1} \\ \theta_i^k \\ a_i^{k+1} \\ a_i^k \end{bmatrix}}_{x_i^{k+1}} &= \underbrace{\begin{bmatrix} 1 & 0 & 0 & 0 & 0 & 0 & 0 \\ 0 & 1 & 0 & 0 & 0 & 0 & 0 \\ 0 & 0 & 1 & 0 & 0 & 0 & 0 \\ 0 & 0 & 0 & 1 + K_\theta & 0 & 0 & 0 \\ 0 & 0 & 0 & 1 & 0 & 0 & 0 \\ 0 & 0 & 0 & 0 & 0 & 1 + K_a & 0 \\ 0 & 0 & 0 & 0 & 0 & 1 & 0 \end{bmatrix}}_{A_i} \underbrace{\begin{bmatrix} \delta_i^k \\ \sigma_i^k \\ u_i^k \\ \theta_i^{k-1} \\ \theta_i^k \\ a_i^k \\ a_i^{k-1} \end{bmatrix}}_{x_i^k} \\ &+ \underbrace{\begin{bmatrix} \mathbf{0}_{3 \times 2} \\ -K_\theta & 0 \\ 0 & 0 \\ 0 & -K_a \\ 0 & 0 \end{bmatrix}}_{B_{u,i}} \underbrace{\begin{bmatrix} \theta_{i,r}^k \\ a_{i,r}^k \end{bmatrix}}_{u_i^k} \\ &+ \underbrace{\begin{bmatrix} c_{1,i} c_{2,i} \bar{a}_{u,i} & -c_{1,i} c_{2,i} \bar{a}_{u,i} & 0 & 0 \\ 0 & 0 & c_{3,i} & -c_{3,i} \\ 0 & 0 & c_{6,i} & -c_{6,i} \\ \mathbf{0}_{4 \times 4} \end{bmatrix}}_{B_{v,i}} \underbrace{\begin{bmatrix} \theta_{i,u}^{k-N} \\ \theta_{i,u}^{k-N-1} \\ a_{i,u}^{k-N} \\ a_{i,u}^{k-N-1} \end{bmatrix}}_{v_i^k} \end{aligned} \quad (27)$$

The downstream effect equation z_i^k from (26) and its matrices $C_{z,i}$ and $D_{z,i}$ are defined as:

$$\underbrace{\begin{bmatrix} \theta_i^k & \theta_i^{k-1} & a_i^k & a_i^{k-1} \end{bmatrix}^T}_{z_i^k} = \underbrace{\begin{bmatrix} \mathbf{0}_{4 \times 3} & \mathbf{I}_{4 \times 4} \end{bmatrix}}_{C_{z,i}} x_i^k + \underbrace{\begin{bmatrix} \mathbf{0}_{4 \times 2} \end{bmatrix}}_{D_{z,i}} u_i^k \quad (29)$$

During the optimization, the predicted values of y_i , z_i , and v_i will be generated along the prediction horizon of length N_p . These predictions can be stacked to provide the vectors Y_i , Z_i , and V_i . Stacking the V_i and Z_i vectors across all the subsystems and constructing an interconnection matrix, Γ , that correctly captures the coupling between systems, upstream and downstream vectors can be related as $\mathbf{V} = \Gamma \mathbf{Z}$. For the wind farm layout simulated in this paper, and assuming no change in the wind direction, the interconnections are:

$$\begin{bmatrix} V_1 \\ V_2 \\ V_3 \\ V_4 \\ V_5 \\ V_6 \end{bmatrix} = \begin{bmatrix} 0 & 0 & 0 & 0 & 0 & 0 \\ I & 0 & 0 & 0 & 0 & 0 \\ 0 & I & 0 & 0 & 0 & 0 \\ 0 & 0 & 0 & 0 & 0 & 0 \\ 0 & 0 & 0 & I & 0 & 0 \\ 0 & 0 & 0 & 0 & I & 0 \end{bmatrix} \begin{bmatrix} Z_1 \\ Z_2 \\ Z_3 \\ Z_4 \\ Z_5 \\ Z_6 \end{bmatrix} \quad (30)$$

where 0 and I are block matrices of appropriate dimension.

B. Subsystem Models with Prediction Horizon

As the subsystems described in (26) are used along the prediction horizon, the predicted output values of Y_i and Z_i

can be represented as:

$$Y_i = F_{y,i}x_i^k + M_{y,i}U_i + N_{y,i}V_i \quad (31)$$

$$Z_i = F_{z,i}x_i^k + M_{z,i}U_i + N_{z,i}V_i \quad (32)$$

where the system matrices F , M , and N are defined in [17].

C. Cost Function and Optimization

The cost function for the LC-DMPC algorithm has the standard quadratic error and control terms, but to facilitate the cooperation between the subsystems and the convergence to the centralized solution, an additional term, $\psi_i^T Z_i$, is added. This term scales with the sensitivities, ψ , that correlate with the interactions between the subsystems. The distributed optimization can be stated as:

$$\begin{aligned} \min_{U_i} J_i &= e_i^T Q_i e_i + U_i^T S_i U_i + \psi_i^T Z_i \\ \text{s.t. (39), (40), \& } U_{i,min} &\leq U_i \leq U_{i,max} \end{aligned} \quad (33)$$

where e_i is the error from the power tracking signal, Q_i is the weight penalizing the error term, U_i are the control actions, S_i is the weight penalizing the control term, ψ_i is the penalty passed from the downstream system, and Z_i is the vector of disturbing inputs to the downstream system.

Quadratic programming can be used to solve the optimization after reformulating the problem to:

$$\begin{aligned} \min_{U_i} J_i &= U_i^T H_i U_i + 2U_i^T F_i + V_i^T E_i V_i + 2V_i^T T_i \\ A_{i,lim} U_i &\leq B_{i,lim} \end{aligned} \quad (34)$$

where

$$\begin{aligned} H_i &= M_{y,i}^T Q_i M_{y,i} + S_i, \quad E_i = N_{y,i}^T Q_i N_{y,i} \\ F_i &= M_{y,i}^T [F_{y,i}x_i^k + N_{y,i}V_i + r_i^k] + 0.5M_{z,i}^T \psi_i \\ T_i &= N_{y,i}^T Q_i [F_{y,i}x_i^k - r_i^k] + 0.5N_{z,i}^T \psi_i \\ A_{i,lim} &= [I_{N_p}, -I_{N_p}]^T, \quad B_{i,lim} = [U_{i,min}^T U_{i,max}^T]^T \end{aligned}$$

The term ψ_i in the optimization comes from the sensitivity of the downstream system to the upstream system's decisions. For example, if the current subsystem i is downstream of the subsystem $i-1$, the sensitivity, γ_i , is computed as the sensitivity of the downstream system's cost function to the upstream disturbance vector.

$$\gamma_i = \frac{\partial J_i}{\partial V_i} = 2 [E_{i-1}V_i + T_i + N_{y,i}^T Q_i M_{y,i}U_i] \quad (35)$$

Stacking these vectors of γ_i , the communication of the sensitivities to the upstream systems as inputs ψ_i can be described with the interconnection matrix as $\psi = \Gamma\gamma$.

In order to ensure convergence of the communication dynamics, a convex combination of the control action is used, given by:

$$u^{k+1} = wu^k + (1-w)u_{QP}^k \quad (36)$$

where u_{QP} is the optimal control action determined by the quadratic program and $w \in [0,1)$ is a tuning parameter. For more information and a proof of stability, see [17].

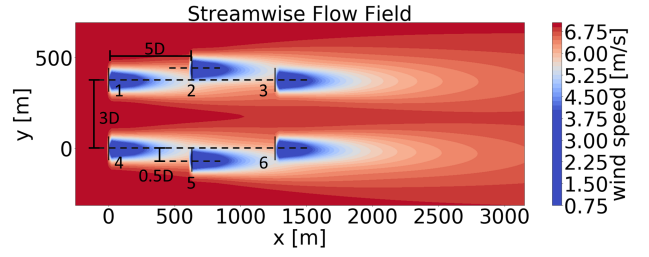


Fig. 2. Simulation of the wakes with FLORIS, showing the layout of the turbines given in [12].

IV. SIMULATION

Simulations of the control method were performed using the same wind farm layout shown in Fig. 2 from [12], as it provides for varying wake conditions in contrast to a regular grid. The simulation environment is a nonlinear dynamic model using a modified FLORIS model [23]. In particular, FLORIS was modified to include the dynamics of the aerodynamic interactions by including a time delay between turbines. The wake of the turbines is assumed to propagate with $\tau = 52$ s, as shown in (8), which is based on Taylor's frozen turbulence hypothesis [20]. The free stream velocity was set to be 12.0 m/s. The linearization points were set around an axial induction factor of 0.15, a yaw misalignment of 0° , a wake deflection of 0 m, a wake half-width of 79.2 m, and wind velocities as determined by FLORIS at each turbine. The axial induction had to be reduced so that there is room for the wind farm power to fluctuate up and down with the AGC signal. The specific AGC signal used in the simulations is the RegD signal defined by the PJM Interconnection [24], a regional transmission organization located in the eastern United States. The RegD signal is a quickly changing signal used by PJM for APC qualification. The signal is 40 minutes long and was up-sampled to the simulation's timestep τ .

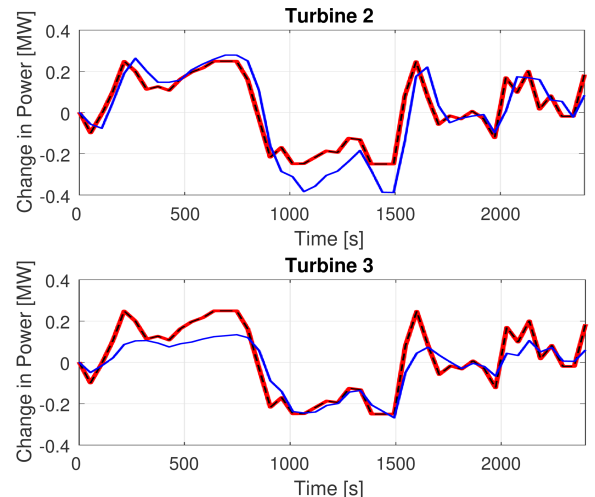


Fig. 3. Results of individual turbines tracking their power reference signals.

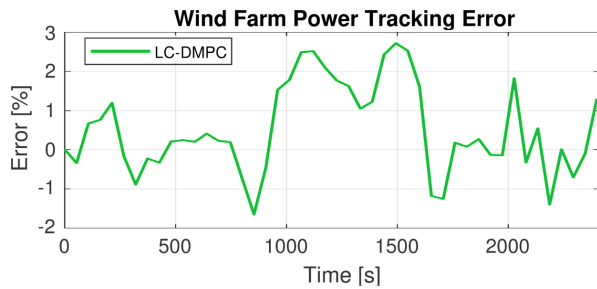


Fig. 4. The wind farm power tracking error.

V. RESULTS

Preliminary results from the simulations verifying AGC tracking capability of the LC-DMPC approach are shown in Fig. 3. Each of the turbines attempts to track its power reference signal, with two turbines shown due to space constraints. The predicted output from the LC-DMPC follows the reference very well while the power output from the FLORIS model shows some discrepancies, though for a linear model it shows good promise and tracking at the farm level. The discrepancies are most likely due to the assumptions that were made in the linear model development as this is a highly nonlinear problem.

The overall tracking error is shown in Fig. 4. For this simulation, the maximum tracking error was 2.72%. The authors consider this performance proof of the LC-DMPC approach's potential for APC of wind farms and will pursue advancements through future work as described below.

VI. CONCLUSIONS & FUTURE WORK

This paper presented a linear wake model and distributed control method for the purpose of optimal wind farm control. The model predicts the effects turbines have on one another through wake interactions. The distributed control algorithm solves a local optimization objective at each turbine, greatly reducing the computational burden compared to a centralized optimization on large-scale wind farms. This is a key challenge of implementing real-time control on wind farms and may help take the optimization from infeasible to practical. Preliminary results show the controller's ability to track an arbitrary power reference for the purpose of providing grid services.

In the future, the authors plan to expand the model to include tilt of the turbine rotor to allow for vertical wake steering in addition to horizontal wake steering. Also, the inclusion of uncertainty in the wind is an important subject to offset some of the simplifications due to the linearizations. The authors would also like to implement an estimator to help address some of the model error seen in the results.

ACKNOWLEDGMENT

The authors would like to thank Vlaho Petrović, Rawand Jalal, and Bryan Rasmussen for valuable discussions about the wind farm control problem and the LC-DMPC approach.

REFERENCES

- [1] Global Wind Energy Council, "Global Wind Report - Annual Market Update," Tech. Rep., 2017.
- [2] E. A. Bossanyi, "Wind Turbine Control for Load Reduction," *Wind Energy*, vol. 6, no. 3, pp. 229–244, July 2003.
- [3] S. Boersma, B. M. Doekemeijer, P. M. O. Gebraad, P. A. Fleming, J. Annoni, A. K. Scholbrock, J. A. Frederik, and J. W. v. Wingerden, "A tutorial on control-oriented modeling and control of wind farms," in *2017 American Control Conference (ACC)*, May 2017, pp. 1–18.
- [4] K. E. Johnson and N. Thomas, "Wind farm control: Addressing the aerodynamic interaction among wind turbines," in *American Control Conference*, June 2009, pp. 2104–2109.
- [5] C. Santoni, U. Ciri, M. Rotea, and S. Leonardi, "Development of a high fidelity CFD code for wind farm control," in *American Control Conference*, July 2015, pp. 1715–1720.
- [6] P. Fleming, P. M. Gebraad, S. Lee, J.-W. van Wingerden, K. Johnson, M. Churchfield, J. Michalakes, P. Spalart, and P. Moriarty, "Simulation comparison of wake mitigation control strategies for a two-turbine case," *Wind Energy*, vol. 18, no. 12, pp. 2135–2143, Dec. 2015.
- [7] P. M. O. Gebraad, "Data-driven wind plant control," Ph.D. dissertation, Delft University of Technology, Delft, The Netherlands, Dec. 2014.
- [8] J. Aho, A. Bucksan, L. Pao, and P. Fleming, "Active power control system for wind turbines capable of primary and secondary frequency control for supporting grid reliability," in *Proceedings of 51st AIAA Aerospace Sciences Meeting*, New York, NY, Jan. 2013.
- [9] P. Fleming, J. Aho, P. Gebraad, L. Pao, and Y. Zhang, "Computational fluid dynamics simulation study of active power control in wind plants," in *American Control Conference*, July 2016, pp. 1413–1420.
- [10] J.-W. van Wingerden, L. Pao, J. Aho, and P. Fleming, "Active power control of waked wind farms," *Preprints of the International Federation of Automatic Control World Congress*, July 2017.
- [11] N. Gionfra, H. Siguerdidjane, G. Sandou, and D. Faille, "Hierarchical control of a wind farm for wake interaction minimization," *IFAC-PapersOnLine*, vol. 49, no. 27, pp. 330–335, Jan. 2016.
- [12] M. Vali, V. Petrovic, S. Boersma, J.-W. v. Wingerden, and M. Kuhn, "Adjoint-based model predictive control of wind farms: Beyond the quasi steady-state power maximization," *Preprints of the International Federation of Automatic Control World Congress*, July 2017.
- [13] J. P. Goit and J. Meyers, "Optimal control of energy extraction in wind-farm boundary layers," *Journal of Fluid Mechanics*, vol. 768, pp. 5–50, Apr. 2015.
- [14] C. R. Shapiro, J. Meyers, C. Meneveau, and D. F. Gayme, "Wind farms providing secondary frequency regulation: Evaluating the performance of model-based receding horizon control," *Journal of Physics: Conference Series*, vol. 753, no. 5, p. 052012, 2016.
- [15] V. Spudić, C. Conte, M. Baotić, and M. Morari, "Cooperative distributed model predictive control for wind farms," *Optimal Control Applications and Methods*, vol. 36, no. 3, pp. 333–352, May 2015.
- [16] M. Soleimanzadeh, R. Wisniewski, and K. Johnson, "A distributed optimization framework for wind farms," *Journal of Wind Engineering and Industrial Aerodynamics*, vol. 123, pp. 88–98, Dec. 2013.
- [17] R. E. Jalal and B. P. Rasmussen, "Limited-communication distributed model predictive control for coupled and constrained subsystems," *IEEE Transactions on Control Systems Technology*, vol. 25, no. 5, pp. 1807–1815, Sept. 2017.
- [18] A. Jiménez, A. Crespo, and E. Migoya, "Application of a LES technique to characterize the wake deflection of a wind turbine in yaw," *Wind Energy*, vol. 13, no. 6, pp. 559–572, Sept. 2010.
- [19] T. Burton, D. Sharpe, N. Jenkins, and E. Bossanyi, *Wind Energy Handbook*. John Wiley & Sons, Dec. 2001.
- [20] G. I. Taylor, "The spectrum of turbulence," *Proceedings of the Royal Society of London A: Mathematical, Physical and Engineering Sciences*, vol. 164, no. 919, pp. 476–490, Feb. 1938.
- [21] M. Bastankhah and F. Porté-Agel, "Experimental and theoretical study of wind turbine wakes in yawed conditions," *Journal of Fluid Mechanics*, vol. 806, pp. 506–541, Nov. 2016.
- [22] N. Jensen, "A note on wind generator interaction," Risø National Laboratory, Report 87-550-0971-9, 1983.
- [23] P. M. O. Gebraad, F. W. Teeuwisse, J. W. van Wingerden, P. A. Fleming, S. D. Ruben, J. R. Marden, and L. Y. Pao, "Wind plant power optimization through yaw control using a parametric model for wake effects - a CFD simulation study," *Wind Energy*, vol. 19, no. 1, pp. 95–114, Jan. 2016.
- [24] PJM, "Ancillary Services." [Online]. Available: <http://www.pjm.com/>